

Light quark mass effects in the on-shell renormalization constants

S. Bekavac^(a), A. Grozin^(b), D. Seidel^(a) and M. Steinhauser^(a)

*(a) Institut für Theoretische Teilchenphysik, Universität Karlsruhe (TH),
76128 Karlsruhe, Germany*

*(b) Budker Institute of Nuclear Physics,
Novosibirsk 630090, Russia*

Abstract

We compute the three-loop relation between the pole and the minimally subtracted quark mass allowing for virtual effects from a second massive quark. We also consider the analogue effects for the on-shell wave function renormalization constant.

PACS numbers: 12.38.Bx 12.38.-t 14.65.Dw 14.65.Fy

1 Introduction

Quark masses are fundamental parameters of the Standard Model (SM) and thus it is desirable to determine their numerical values with the highest possible precision. In order to do so it is necessary to fix a renormalization scheme which defines the quark mass. A renormalization scheme which is of particular importance in those situations where the quark mass is small as compared to the typical energy scale is the $\overline{\text{MS}}$ scheme. Although it has no immediate physical interpretation, in general a good convergence in perturbation theory is observed. On the other hand, the most intuitive renormalization scheme is the on-shell scheme where the renormalized quark mass is defined as the pole of the propagator. It is well known that such a definition is plagued by numerically large long-distance effects which are connected to the renormalon corrections. As a consequence one observes a bad behaviour of the perturbative expansion if the pole mass is used as a parameter. Still, it plays a crucial role in all computations of threshold phenomena like energy levels or the decay of a quark-anti-quark bound state. In order to make contact between high-energy phenomena on one side and threshold processes on the other side it is necessary to have a precise relation between the pole and the $\overline{\text{MS}}$ quark mass at hand. Important three-loop contributions are provided in this paper. As a by-product we also compute the same kind of corrections to the wave function renormalization constant.

The one-loop corrections to the relation between the $\overline{\text{MS}}$ and on-shell mass have been computed almost 30 years ago in Ref. [1]. About ten years later, the two-loop corrections have been calculated in Ref. [2]. Shortly afterwards also the two-loop result for the on-shell wave function renormalization constant Z_2^{OS} has been obtained [3]. Contributions with a single mass scale were expressed via master integrals exactly in $d = 4 - 2\varepsilon$; the ε -expansion of the only non-trivial master integral is known [4, 5] far enough to obtain $\mathcal{O}(\varepsilon^4)$ terms in Z_m^{OS} and Z_2^{OS} . Contributions with two mass scales were obtained up to $\mathcal{O}(1)$ only. Later, a reduction algorithm for two-loop two-scale on-shell integrals has been constructed, and expressions via master integrals exact in d have been obtained [6].¹ The three-loop relation between the $\overline{\text{MS}}$ and on-shell mass has been computed at the end of the nineties in a semi-numerical way in Refs. [9, 10] where the off-shell fermion propagator has been considered for small and large external momenta. The on-shell quantities have been obtained with the help of a conformal mapping and Padé approximation. Later the results have been confirmed in Ref. [11] by an analytical on-shell calculation. The three-loop result for Z_2^{OS} has been obtained in Ref. [12]. Both analytical calculations have recently been rederived in Ref. [13]. In this paper we complete the three-loop results for the mass counterterm Z_m^{OS} and Z_2^{OS} by computing the contributions where a second mass scale is present through a closed quark loop. We would like to mention that the approximation linear in the mass ratio has been derived in Ref. [14] using the corresponding corrections to the static potential [15] and their cancellation in the relation between the $\overline{\text{MS}}$ and 1S

¹The ε -expansion of the two non-trivial master integrals was only obtained up to $\mathcal{O}(1)$. One of these integrals was later expanded to $\mathcal{O}(\varepsilon^5)$ [7] (though only the $\mathcal{O}(\varepsilon)$ term is published). Both integrals were calculated [8] up to $\mathcal{O}(\varepsilon)$, as series in the mass ratio up to the sixth order.

quark mass.

We concentrate on the situation where the second quark mass is smaller than the external one, although our formulae can also be applied to the reversed situation. Then, however, often it is advantageous to perform a decoupling of the heavy mass leading to an effective theory where the latter is integrated out.

As far as the quark masses in the SM are concerned the corrections considered in this paper are of practical relevance for the bottom quark where the second mass scale is given by the charm quark. In this case we have for the mass ratio $m_c/m_b \approx 0.3$. Thus the massless approximation does not provide a good result. In all other cases the effect from a lighter quark mass is negligible. Nevertheless, below generic results are presented.

In principle at three-loop order there is also a contribution involving two additional masses which are present in two closed fermion loops. However, for all practical applications the lightest quark mass can safely be neglected.

The remainder of the paper is organized as follows: In Section 2 we discuss the framework which is used for the calculation. Afterwards the results for the relation between the on-shell and $\overline{\text{MS}}$ quark mass and the wave function renormalization constant are discussed in Sections 3 and 4, respectively. Since the analytical expressions are quite involved we present in both cases handy approximation formulae of our results. Finally, Section 5 contains a simple application and our conclusions. Appendix A lists all master integrals in graphical form.

2 On-shell renormalization of quark mass and wave function

The formulae relevant for the computation of the renormalization constants for the mass and wave function have been derived in Refs. [12, 13]. For completeness we repeat the resulting expressions which read

$$Z_m^{\text{OS}} = 1 + \Sigma_1(M_q^2, M_q), \quad (1)$$

$$(Z_2^{\text{OS}})^{-1} = 1 + 2M_q^2 \frac{\partial}{\partial q^2} \Sigma_1(q^2, M_q) \Big|_{q^2=M_q^2} + \Sigma_2(M_q^2, M_q), \quad (2)$$

where Z_m^{OS} and Z_2^{OS} are defined through

$$m_{q,0} = Z_m^{\text{OS}} M_q, \quad (3)$$

$$\psi_0 = \sqrt{Z_2^{\text{OS}}} \psi. \quad (4)$$

ψ is the quark field renormalized in the on-shell scheme with mass m_q , M_q is the on-shell mass and bare quantities are denoted by a subscript 0. Σ denotes the quark self-energy

contributions which can be decomposed as

$$\Sigma(q, m_q) = m_q \Sigma_1(q^2, m_q) + (\not{q} - m_q) \Sigma_2(q^2, m_q). \quad (5)$$

For completeness let us also introduce the $\overline{\text{MS}}$ renormalization constant via

$$m_{q,0} = Z_m^{\overline{\text{MS}}} m_q(\mu). \quad (6)$$

The quantities on the right-hand side of Eqs. (1) and (2) are obtained by considering the external momentum of the quarks to be $q = Q(1+t)$ with $Q^2 = M_q^2$. The application of the projector $(\not{Q} + M_q)/(4M_q^2)$ and an expansion to first order in t leads to

$$\begin{aligned} \text{Tr} \left\{ \frac{\not{Q} + M_q}{4M_q^2} \Sigma(q, M_q) \right\} &= \Sigma_1(q^2, M_q) + t \Sigma_2(q^2, M_q) \\ &= \Sigma_1(M_q^2, M_q) + \left(2M_q^2 \frac{\partial}{\partial q^2} \Sigma_1(q^2, M_q) \Big|_{q^2=M_q^2} + \Sigma_2(M_q^2, M_q) \right) t \\ &\quad + \mathcal{O}(t^2). \end{aligned} \quad (7)$$

Thus, to obtain Z_m^{OS} one only needs to calculate Σ_1 for $q^2 = M_q^2$. To calculate Z_2^{OS} , one has to compute the first derivative of the self-energy diagrams. The mass renormalization is taken into account iteratively by calculating one- and two-loop diagrams with zero-momentum insertions.

The results for the renormalization constants can be cast into the following form

$$\begin{aligned} Z_i^{\text{OS}} &= 1 + \frac{\alpha_s(\mu)}{\pi} \left(\frac{e^{\gamma_E}}{4\pi} \right)^{-\varepsilon} \delta Z_i^{(1)} + \left(\frac{\alpha_s(\mu)}{\pi} \right)^2 \left(\frac{e^{\gamma_E}}{4\pi} \right)^{-2\varepsilon} \delta Z_i^{(2)} \\ &\quad + \left(\frac{\alpha_s(\mu)}{\pi} \right)^3 \left(\frac{e^{\gamma_E}}{4\pi} \right)^{-3\varepsilon} \delta Z_i^{(3)} + \mathcal{O}(\alpha_s^4), \end{aligned} \quad (8)$$

with $i \in \{m, 2\}$. It is convenient to further decompose the two- and three-loop contribution in terms of the different colour factors

$$\begin{aligned} \delta Z_i^{(2)}(x) &= C_F^2 Z_i^{FF} + C_F C_A Z_i^{FA} + C_F T_F n_l Z_i^{FL} + C_F T_F n_h Z_i^{FH} + C_F T_F n_m Z_i^{FM}(x) \\ \delta Z_i^{(3)}(x) &= C_F^3 Z_i^{FFF} + C_F^2 C_A Z_i^{FFA} + C_F C_A^2 Z_i^{FAA} + C_F T_F n_l (C_F Z_i^{FFL} + C_A Z_i^{FAL} \\ &\quad + T_F n_l Z_i^{FLL} + T_F n_h Z_i^{FHL} + T_F n_m Z_i^{FML}(x)) \\ &\quad + C_F T_F n_h (C_F Z_i^{FFH} + C_A Z_i^{FAH} + T_F n_h Z_i^{FHH} + T_F n_m Z_i^{FMH}(x)) \\ &\quad + C_F T_F n_m (C_F Z_i^{FFM}(x) + C_A Z_i^{FAM}(x) + T_F n_m Z_i^{FMM}(x)), \end{aligned} \quad (9)$$

where n_l and n_h mark the closed quark loops with mass zero and m_q , respectively. n_m labels the closed quark loops involving a second mass scale which we denote as m_f . Although we have $n_h = 1$ and $n_m = 1$ in our applications, we keep a generic label which is useful when tracing the origin of the individual contributions. In Eq. (9) $C_F =$

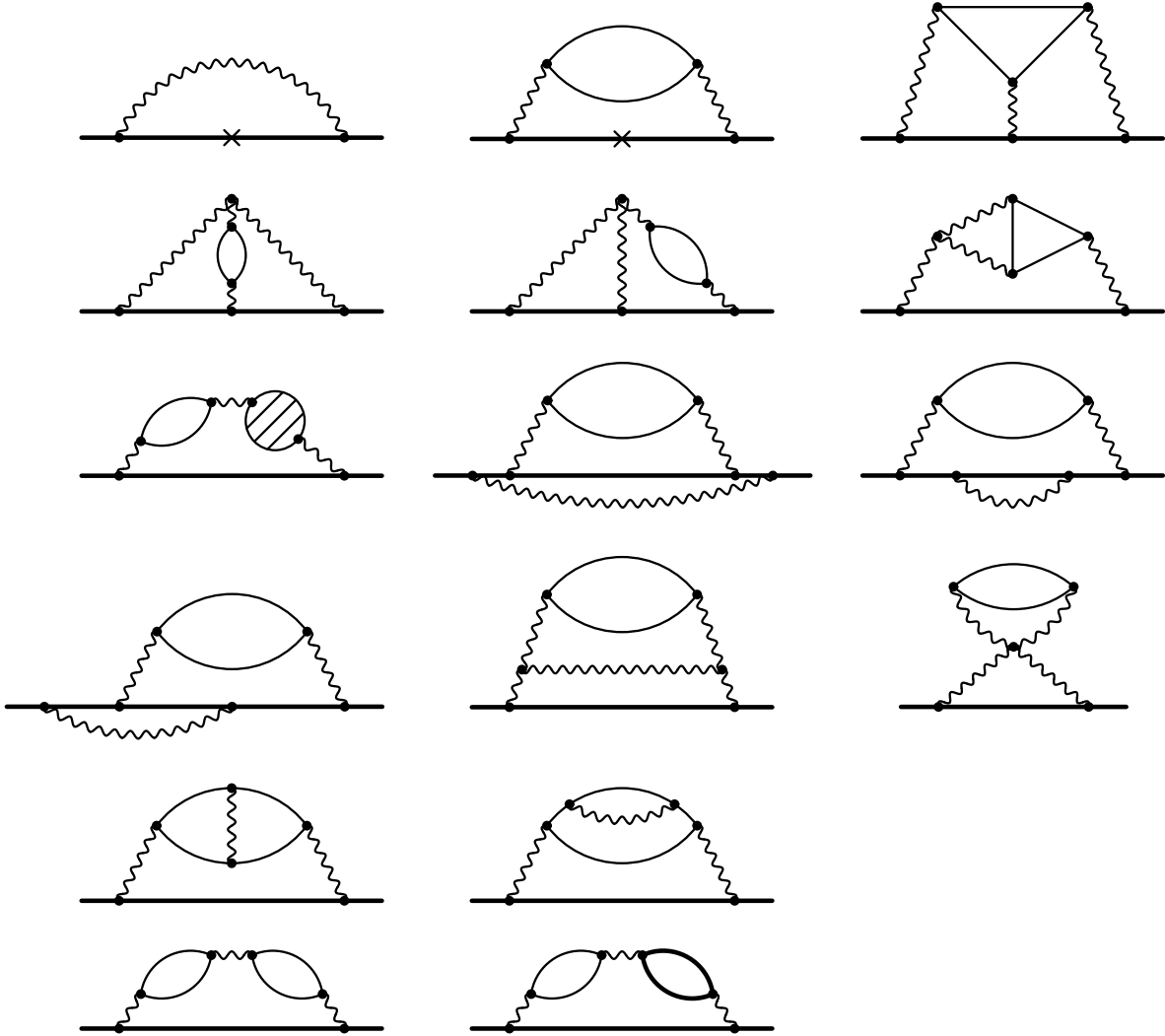


Figure 1: All three-loop heavy-quark self-energy diagrams containing n_m . Thick solid lines denote massive quarks with mass m_q and thin ones quarks with mass m_f . Wavy lines denote gluons and crosses mark counterterm insertions. The shaded blob denotes the sum of one-loop massless self-energy insertions (massless quarks, gluons, ghosts).

$(N_c^2 - 1)/(2N_c)$ and $C_A = N_c$ are the eigenvalues of the quadratic Casimir operators of the fundamental and adjoint representation of $SU(N_c)$, respectively. In the case of QCD we have $N_c = 3$. $T_F = 1/2$ is the index of the fundamental representation and $n_f = n_l + n_h + n_m$ is the number of quark flavours. $\alpha_s(\mu)$ is the strong coupling constant defined in the $\overline{\text{MS}}$ scheme with n_f active flavours. The coefficients proportional to n_m are

functions of the mass ratio which we define by

$$x = \frac{M_f}{M_q}, \quad (10)$$

i.e. the ratio of the on-shell masses. The dependence of the coefficients in Eq. (9) on $L_\mu = \log \mu^2/M_q^2$ is suppressed. The Feynman diagrams producing n_m -dependent contributions to Z_m^{OS} and Z_2^{OS} are shown in Fig. 1.

The one-loop result for Z_m^{OS} expanded up to order ε^2 can be found in Eq. (13) of Ref. [13] and the expression for $\delta Z_m^{(2)}|_{n_m=0}$ including $\mathcal{O}(\varepsilon)$ terms is given in Eq. (14) of the same reference. Z_m^{FM} and Z_2^{FM} have been computed in analytic form in Ref. [2]. The main result of this paper are the functions Z_m^{FFM} , Z_m^{FAM} , Z_m^{FLM} , Z_m^{FHM} and Z_m^{FMM} which are discussed in Section 3.

In the case of the mass renormalization it is convenient to consider the ratio between the on-shell and $\overline{\text{MS}}$ renormalization constants

$$z_m = \frac{Z_m^{\text{OS}}}{Z_m^{\overline{\text{MS}}}} = \frac{m_q}{M_q} \quad (11)$$

which is finite. We furthermore adopt the notation introduced in Eqs. (8) and (9) for Z_m^{OS} also for z_m . Let us for later reference provide already here the result for the $\overline{\text{MS}}$ renormalization constant which is given by [16]

$$Z_m^{\overline{\text{MS}}} = 1 + \sum_{i=1}^{\infty} C_i \left(\frac{\alpha_s(\mu)}{\pi} \right)^i, \quad (12)$$

with

$$\begin{aligned} C_1 &= -\frac{1}{\varepsilon}, \\ C_2 &= \frac{1}{\varepsilon^2} \left(\frac{15}{8} - \frac{1}{12} n_f \right) + \frac{1}{\varepsilon} \left(-\frac{101}{48} + \frac{5}{72} n_f \right), \\ C_3 &= \frac{1}{\varepsilon^3} \left(-\frac{65}{16} + \frac{7}{18} n_f - \frac{1}{108} n_f^2 \right) + \frac{1}{\varepsilon^2} \left(\frac{2329}{288} - \frac{25}{36} n_f + \frac{5}{648} n_f^2 \right) \\ &\quad + \frac{1}{\varepsilon} \left(-\frac{1249}{192} + \frac{5}{18} \zeta_3 n_f + \frac{277}{648} n_f + \frac{35}{3888} n_f^2 \right). \end{aligned} \quad (13)$$

As far as the wave function renormalization constant is concerned, we have at the one-loop level $\delta Z_2^{(1)} = \delta Z_m^{(1)}$ and the two-loop contributions for $n_m = 0$, including order ε terms, can be found in Eq. (25) of Ref. [13]. The results for the functions Z_2^{FFM} , Z_2^{FAM} , Z_2^{FLM} , Z_2^{FHM} and Z_2^{FMM} are discussed in Section 4.

Starting from the three-loop level, the wave function renormalization constant depends on the gauge parameter, ξ , which we define through the gluon propagator as

$$D_{\mu\nu}^{ab}(k) = -\frac{i}{k^2} \left(g_{\mu\nu} - \xi \frac{k_\mu k_\nu}{k^2} \right) \delta^{ab}, \quad (14)$$

where a and b are colour indices.

3 On-shell mass relation

3.1 Two-loop result

Before discussing in detail the three-loop result let us consider the two-loop quantity z_m^{FM} . The analytical result can be found in Ref. [2] and is given by

$$\begin{aligned}
 z_m^{FM} = & \frac{1}{96} \left\{ 48x^4 \log^2(x) + 48x^2 \log(x) + 72x^2 + 4L_\mu(3L_\mu + 13) \right. \\
 & + 8\pi^2 (x^4 - 3x^3 - 3x + 1) + 71 \\
 & - 48(x+1)^2 (x^2 - x + 1) [\log(x) \log(x+1) + \text{Li}_2(-x)] \\
 & \left. - 48(x-1)^2 (x^2 + x + 1) [\log(x) \log(1-x) + \text{Li}_2(x)] \right\}, \quad (15)
 \end{aligned}$$

where $L_\mu = \log(\mu^2/M_q^2)$ and Li_2 is the dilogarithm. In our approach all occurring integrals are reduced to four master integrals [6]. The Harmonic Polylogarithms (HPL) [17] which appear in a first step in the results of these integrals can be transformed into the (di)logarithms of Eq. (15) resulting in complete agreement with Ref. [2].²

In Fig. 2 z_m^{FM} is shown as a function of x for $\mu^2 = M_q^2$. In addition to the exact result we also show the curves corresponding to the linear approximations for $x \rightarrow 0$ and $x \rightarrow 1$. One observes a rapid convergence of both expansions which almost extends to $x = 1$ ($x = 0$) once the x^{10} ($(1-x)^{10}$) terms are included. Note that the x^5 terms are sufficient in order to provide an excellent approximation far below the per mill level for $x = 0.3$. We also want to mention that a 12% deviation is observed (for $x = 0.3$) if only the linear terms in x are included into the expansion.

Let us finally provide an approximation formula [2] which agrees to better than 1% with the analytical formula of Eq. (15):

$$\tilde{z}_m^{FM} = 1.562 - 2.394x + 0.9428x^2 - 0.2666x^3 + \frac{13}{24}L_\mu + \frac{1}{8}L_\mu^2. \quad (16)$$

3.2 Three-loop corrections

At three-loop order we want to discuss in a first step the coefficients of the five n_m -dependent colour structures but afterwards also consider the physical quantity which is obtained after inserting the numerical values for the QCD colour factors.

All Feynman diagrams are generated with QGRAF [18] and the various topologies are identified with the help of q2e and exp [19,20]. In a second calculation the three-loop diagrams were generated starting from three generic topologies which already appear in the calculation of Ref. [21]. In a next step the reduction of the various functions to so-called master integrals (MI's) has to be achieved. For this step we use the so-called Laporta

²A trivial overall factor $C_F = 4/3$ is actually missing in Eqs. (17) and (20) of this reference.

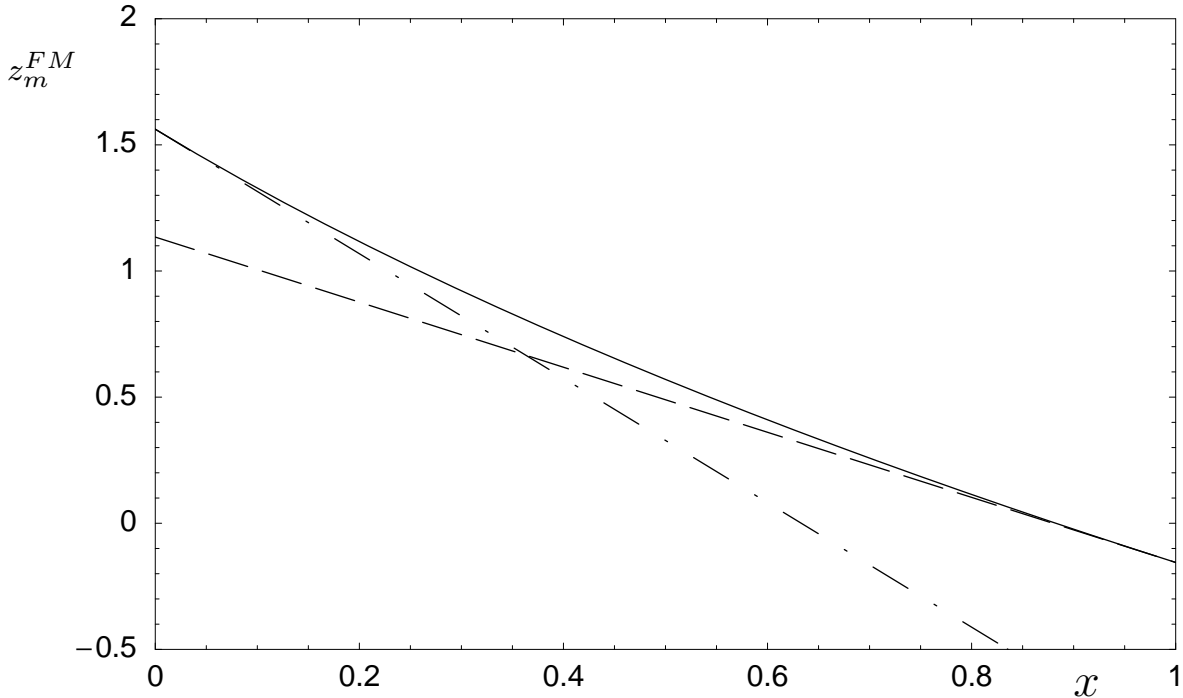


Figure 2: The two-loop correction z_m^{FM} as a function of x at $\mu = M_q$. Next to the exact result (solid line) also the approximations for $x \rightarrow 0$ (dash-dotted line) and for $x \rightarrow 1$ (dashed line) are shown including the linear terms.

method [22, 23] which reduces the three-loop integrals to 27 MI's. We use the implementation of Laporta's algorithm in the program **Crusher** [24]. It is written in **C++** and uses **GiNaC** [25] for simple manipulations like taking derivatives of polynomial quantities. In the practical implementation of the Laporta algorithm one of the most time-consuming operations is the simplification of the coefficients appearing in front of the individual integrals. This task is performed with the help of **Fermat** [26] where a special interface has been used (see Ref. [27]). The main features of the implementation are the automated generation of the integration-by-parts (IBP) identities [28], a complete symmetrization of the diagrams and the possibility to use multiprocessor environments.

In Figs. 7–10 of Appendix A a graphical representation of the master integrals can be found. We have chosen two independent ways to compute the ε -expansion of the master integrals. The first one relies on the Mellin-Barnes technique (see, e.g., Ref. [29]) and provides us with numerical results. Here we have used the **Mathematica** package **MB.m** [30]. With the help of our second method, based on differential equations, Ref. [31], we were able to evaluate all but four master integrals in analytic form. More details can be found in Ref. [32].

The coefficient functions of all master integrals contain a $1/\varepsilon$ pole, some even a $1/\varepsilon^2$ term which means that the master integrals have to be expanded up to order ε and ε^2 ,

respectively. All but four master integrals could be evaluated analytically in terms of HPLs which we evaluate numerically with the help of the `Mathematica` package `HPL.m` [33, 34]. Two of the remaining four integrals, which are all needed up to order ε , could be computed including the constant term [32] and for the residual two integrals analytical results are obtained for the pole parts. For the still remaining six coefficients integral representations are available which in the worst case are two-dimensional.

Close to $x = 0$ we observe large cancellations between the contributions originating from different master integrals. On the other hand, as we have seen above, the expansion for $x \ll 1$ converges very fast; at two-loop order the first five terms approximate the exact result to 0.02% for $x = 0.3$ which is relevant for the charm mass effects to the bottom quark mass. For this reason we decided to derive an expansion of our result including terms of order x^8 . The results expressed in terms of HPLs can simply be expanded using `HPL.m` [33, 34]. For the remaining coefficients we use their Mellin-Barnes representation in order to express them in terms of multiple sums which in turn leads to the coefficients of x^n .

Our result for the five functions z_m^{FFM} , z_m^{FAM} , z_m^{FLM} , z_m^{FHM} and z_m^{FMM} are shown in Fig. 3 for $0 \leq x \leq 1$. The exact results are represented by thick lines and the expansion terms for $x \rightarrow 0$ up to the linear term as thin lines. The latter provide a good approximation to the exact results up to about $x \approx 0.1 \dots 0.4$, depending on the colour structure. We want to mention that the expansion terms including corrections of order x^8 provide a good approximation almost up to $x = 1$. Note that for $x = 0.3$ the linear approximation deviates from the exact result (obtained by the proper sum of the individual colour structures) by 8%, whereas the deviation including terms up to x^5 is only 0.008%.

The x -dependence of the individual curves is rather flat, in particular close to $x = 1$ — except for z_m^{FAM} . The latter varies from +13.10 for $x = 0$ to -1.52 for $x = 1$ with a zero for $x \approx 0.81$. It is interesting to note that the coefficient of $C_F^2 T n_m$ is positive for $0 \leq x \leq 1$ whereas the contributions originating from the diagrams involving two closed fermion loops are negative and furthermore numerically smaller in a large part of the x interval.

The boundary terms for $x = 0$ and $x = 1$ can be extracted from the known single-scale three-loop results [9–11, 13] and are given by

$$\begin{aligned}
z_m^{FFM}(0) &= z_m^{FLL} \approx 0.842, & z_m^{FFM}(1) &= z_m^{FFH} \approx 2.494, \\
z_m^{FAM}(0) &= z_m^{FAL} \approx 13.099, & z_m^{FAM}(1) &= z_m^{FAH} \approx -1.522, \\
z_m^{FLM}(0) &= 2z_m^{FLL} \approx -3.916, & z_m^{FLM}(1) &= z_m^{FHL} \approx -0.067, \\
z_m^{FHM}(0) &= z_m^{FHL} \approx -0.067, & z_m^{FHM}(1) &= 2z_m^{FHH} \approx -0.384, \\
z_m^{FMM}(0) &= z_m^{FLL} \approx -1.958, & z_m^{FMM}(1) &= z_m^{FHH} \approx -0.192.
\end{aligned} \tag{17}$$

These limits constitute an important cross check of our calculation. We find perfect agreement with the known results.

We refrain from listing explicit results for the x -

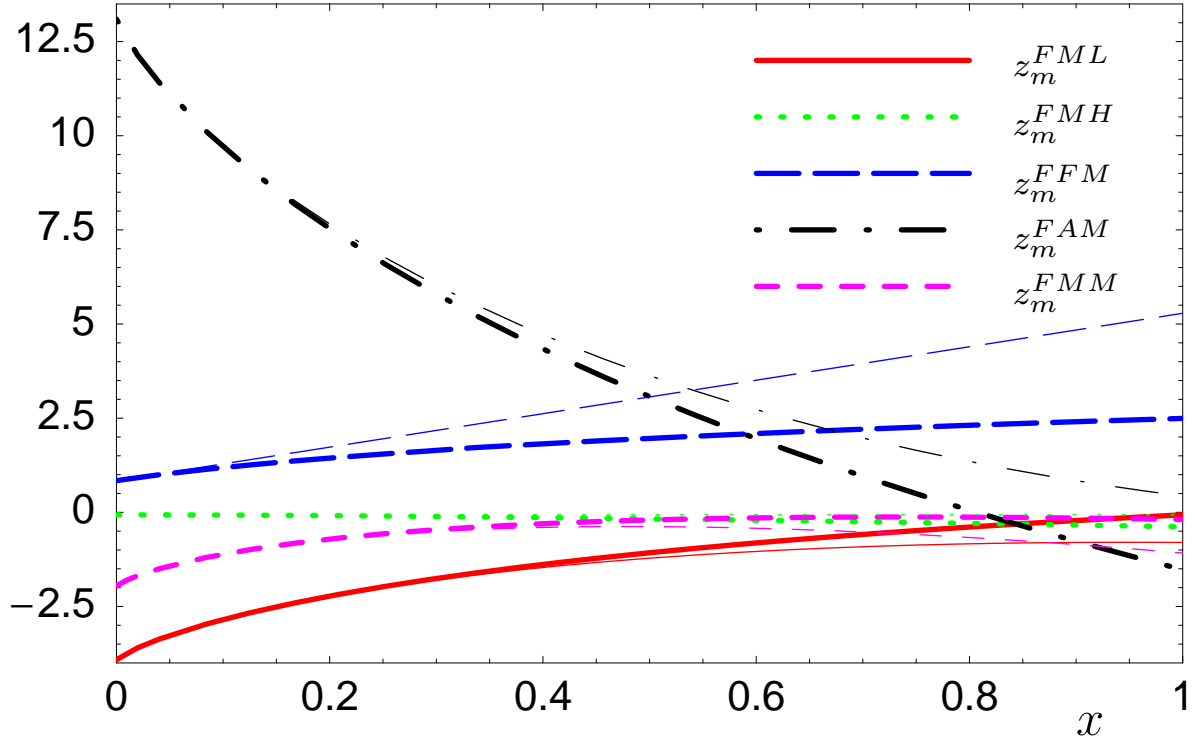


Figure 3: z_m^{FFM} , z_m^{FAM} , z_m^{FLM} , z_m^{FHM} and z_m^{FMM} as a function of x . The exact curves are represented by the thick and the linear approximations for small x by the thin lines.

dependent coefficients which can be obtained at the URL <http://www-ttp.physik.uni-karlsruhe.de/Progdata/ttp07/ttp07-21/>. Instead we provide approximation formulae which have an accuracy of better than 1% for $0 \leq x \leq 1$. They are inspired by the expansion for small values of x and the behaviour for $x = 1$.³ We obtain

$$\begin{aligned}
\tilde{z}_m^{FFM} &= 0.842 + 4.333x - 1.365x^2 + 3.136x^2 \log x - 1.316x^3 \\
&\quad + L_\mu (-0.972 + 1.820x - 0.811x^2 + 0.279x^3) - \frac{13}{32}L_\mu^2 - \frac{3}{32}L_\mu^3, \\
\tilde{z}_m^{FAM} &= 13.099 - 12.945x + 9.041x \log x - 1.676x^2 \\
&\quad + L_\mu (6.724 - 4.407x + 1.807x^2 - 0.549x^3) + \frac{373}{288}L_\mu^2 + \frac{11}{72}L_\mu^3, \\
\tilde{z}_m^{FLM} &= -3.916 + 2.948x - 3.304x \log x + 0.901x^2 \\
&\quad + L_\mu (-1.921 + 1.604x - 0.660x^2 + 0.201x^3) - \frac{13}{36}L_\mu^2 - \frac{1}{18}L_\mu^3, \\
\tilde{z}_m^{FHM} &= -0.067 - 0.612x^2 + 0.443x^3 - 0.148x^4 \\
&\quad + L_\mu (-0.776 + 1.597x - 0.631x^2 + 0.179x^3) - \frac{13}{36}L_\mu^2 - \frac{1}{18}L_\mu^3,
\end{aligned}$$

³We want to mention that the formulae provided on the web page are valid for $0 \leq x \leq 5$.

$$\begin{aligned}
z_m^{FMM} &= -1.958 + 0.501x - 3.403x \log x + 1.264x^2 - 0.103x^3 \log x \\
&\quad + L_\mu \left(-0.960 + 1.600x - 0.653x^2 + 0.198x^3 \right) - \frac{13}{72} L_\mu^2 - \frac{1}{36} L_\mu^3. \quad (18)
\end{aligned}$$

Let us in the following consider the result in the case of QCD, i.e., we set $C_F = 4/3$, $C_A = 3$, $T_F = 1/2$, $n_h = 1$, $n_m = 1$ and define the quantities

$$\begin{aligned}
z_m^{(2),M} &= C_F T_F z_m^{FM}, \quad (19) \\
z_m^{(3),M} &= C_F^2 T_F z_m^{FFM} + C_F C_A T_F z_m^{FAM} + C_F T_F^2 z_m^{FML} + C_F T_F^2 z_m^{FMH} + C_F T_F^2 z_m^{FMM}.
\end{aligned}$$

Evaluating the coefficients for the z -expansion in numerical form the results become very compact and are given by ($\mu^2 = M_q^2$)

$$\begin{aligned}
z_m^{(2),M} &= +x^0 (1.0414) + x^1 (-1.6449) + x^2 (1.0000) + x^3 (-1.6449) \\
&\quad + x^4 (1.2474 - 0.7222L_x + 0.3333L_x^2) + x^6 (-0.0844 + 0.0889L_x) \\
&\quad + x^8 (-0.0118 + 0.0214L_x), \\
z_m^{(3),M} &= +x^0 (26.2712 - 1.3054n_l) \\
&\quad + x^1 (-21.0921 + 16.9977L_x + 1.0385n_l - 1.0966L_x n_l) \\
&\quad + x^2 (12.7021 + 10.6870L_x - 0.2222n_l) \\
&\quad + x^3 (-13.0084 + 16.5103L_x - 0.2408n_l - 1.0966L_x n_l) \\
&\quad + x^4 \left[-4.1035 + 0.1938L_x - 0.2593L_x^3 + 0.7919L_x^2 + n_l (0.3613 - 0.2822L_x \right. \\
&\quad \quad \left. + 0.0741L_x^3 - 0.2407L_x^2) \right] \\
&\quad + x^5 (-1.4908 + 2.8512L_x + 0.4935n_l) \\
&\quad + x^6 (0.1654 - 0.5756L_x + 0.8224L_x^2 - 0.1873n_l + 0.0267L_x n_l) \\
&\quad + x^7 (-0.1751 + 0.5452L_x + 0.0653n_l) \\
&\quad + x^8 \left[-0.0705 + 0.0492L_x + 0.3125L_x^2 + n_l (-0.0377 + 0.0025L_x) \right], \quad (20)
\end{aligned}$$

where the contributions proportional to n_l are listed separately and $L_x = \log x$. In Fig. 4 the expansions of the quantity $z_m^{(3),M}$ up to x^n ($n = 1, 3, 5, 8$) are shown together with the exact expressions where $n_l = 3$ has been chosen corresponding to the case $M_f = M_c$ and $M_q = M_b$. One observes a rapid convergence when including successively higher orders. In Tab. 1 numerical results for the individual coefficient functions, for $z_m^{(3),M}$ and $z_m^{(3)}$ are shown in the region around $x = 0.3$ where again $n_l = 3$ has been adopted.

Quite often it is convenient to consider the masses which only appear in closed loops in the $\overline{\text{MS}}$ scheme. Thus, transforming M_f to the $\overline{\text{MS}}$ scheme leads to the following modifications of Eq. (19):

$$\begin{aligned}
z_m^{(2),M}(x) &\rightarrow z_m^{(2),M}(x_f), \\
z_m^{(3),M}(x) &\rightarrow z_m^{(3),M}(x_f) + C_F^2 T_F n_m \Delta z_m^f(x_f), \quad (21)
\end{aligned}$$

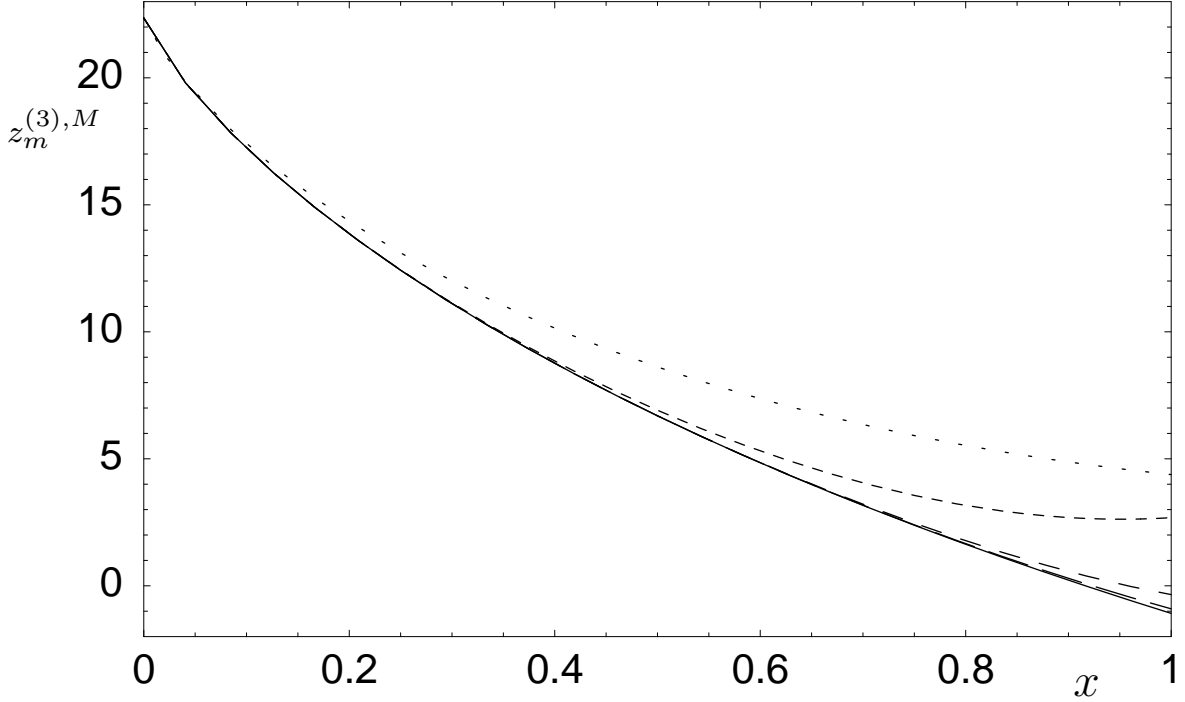


Figure 4: $z_m^{(3),M}$ as a function of x where $n_l = 3$ and $\mu^2 = M_q^2$ has been chosen. The exact result is shown together with the expansions up to x^n ($n = 1, 3, 5, 8$) (dotted line to long-dashed line).

x	z_m^{FFM}	z_m^{FAM}	z_m^{FLM}	z_m^{FHM}	z_m^{FMM}	$z_m^{(3)M}$	$z_m^{(3)}$
0.26	1.57	6.45	-1.93	-0.10	-0.55	12.15	-111.66
0.27	1.59	6.29	-1.89	-0.10	-0.52	11.89	-111.92
0.28	1.61	6.12	-1.84	-0.11	-0.50	11.62	-112.19
0.29	1.63	5.96	-1.80	-0.11	-0.48	11.37	-112.44
0.30	1.64	5.80	-1.76	-0.11	-0.46	11.11	-112.70
0.31	1.66	5.64	-1.72	-0.11	-0.44	10.86	-112.95
0.32	1.68	5.49	-1.68	-0.12	-0.42	10.61	-113.20
0.33	1.70	5.34	-1.64	-0.12	-0.41	10.37	-113.44
0.34	1.72	5.19	-1.60	-0.12	-0.39	10.13	-113.68

Table 1: Numerical results for x -dependent coefficients contributing to the three-loop quantity $z_m^{(3)}$. For the renormalization scale $\mu^2 = M_q^2$ has been adopted.

with

$$x_f \equiv x_f(\mu_f) = \frac{m_f(\mu_f)}{M_q},$$

$$\begin{aligned}
\Delta z_m^f(x_f) &= \frac{1}{24} \left(\frac{3}{2} l_{\mu_f} + 2 \right) x \{ 24x^3 \log^2(x) + 12x \log(x) + 24x \\
&\quad + \pi^2 [x^2(4x - 9) - 3] - 6 [(4x + 3)x^2 + 1] [\log(x) \log(x + 1) + \text{Li}_2(-x)] \\
&\quad - 6(x - 1)(4x^2 + x + 1) [\log(1 - x) \log(x) + \text{Li}_2(x)] \}, \tag{22}
\end{aligned}$$

where $l_{\mu_f} = \log(\mu_f^2/m_f^2)$. In Eq. (22) we introduced the scale μ_f for the renormalization point of the quark mass m_f which is different from μ implicitly present in Eq. (9). The latter contains the information about the running of α_s whereas the former incorporates the anomalous mass dimension of m_f .

Let us for completeness also present the inverse relation $1/z_m$ which is conveniently expressed in terms of the $\overline{\text{MS}}$ quark mass m_q . Using analogous conventions to (19) we find

$$\begin{aligned}
(1/z_m)^{(2),M}(x_q) &= (M_q/m_q(\mu))^{(2),M}(x_q) = -z_m^{(2),M}(x_q) \Big|_{L_\mu \rightarrow l_\mu}, \\
(1/z_m)^{(3),M}(x_q) &= (M_q/m_q(\mu))^{(3),M}(x_q) = -z_m^{(3),M}(x_q) \Big|_{L_\mu \rightarrow l_\mu} + C_F^2 T_F n_m \Delta z_m^q(x_q), \tag{23}
\end{aligned}$$

with

$$\begin{aligned}
x_q &\equiv x_q(\mu) = \frac{M_f}{m_q(\mu)}, \\
\Delta z_m^q(x_q) &= \frac{1}{192} \{ 48(3l_\mu + 7)x_q^4 \log^2(x_q) + 144x_q^2 \log(x_q) + 312x_q^2 \\
&\quad + 8\pi^2 (7x_q^4 - 15x_q^3 - 3x_q - 1) + 137 \\
&\quad - l_\mu \left[-72x_q^2 + 24l_\mu \left(\frac{3}{2} l_\mu + 4 \right) + 12\pi^2 (-2x_q^4 + 3x_q^3 - 3x_q + 2) + 13 \right] \\
&\quad - 48 \left[(7x_q + 5)x_q^3 + x_q + \frac{3}{2} l_\mu (2x_q^4 + x_q^3 - x_q - 2) - 1 \right] \\
&\quad \quad \times [\log(x_q) \log(x_q + 1) + \text{Li}_2(-x_q)] \\
&\quad + 48(x_q - 1) \left[\frac{3}{2} l_\mu (2x_q^3 + x_q^2 + x_q + 2) + 7x_q^3 + 2x_q^2 + 2x_q + 1 \right] \\
&\quad \quad \times [-\log(1 - x_q) \log(x_q) - \text{Li}_2(x_q)] \}. \tag{24}
\end{aligned}$$

It is understood that the renormalization scale dependent logarithms appearing in $z_m^{(2),M}(x_q)$, $z_m^{(3),M}(x_q)$ and $\Delta z_m^q(x_q)$ are defined as $l_\mu = \log(\mu^2/m_q^2)$.

Again we can consider the masses which only appear in closed loops in the $\overline{\text{MS}}$ scheme, which leads to the following modifications of Eq. (23):

$$\begin{aligned}
(1/z_m)^{(2),M}(x_q) &\rightarrow (1/z_m)^{(2),M}(x_{fq}), \\
(1/z_m)^{(3),M}(x_q) &\rightarrow (1/z_m)^{(3),M}(x_{fq}) + C_F^2 T_F n_m \Delta z_m^{fq}(x_{fq}), \tag{25}
\end{aligned}$$

with

$$\begin{aligned}
x_{fq} &\equiv x_{fq}(\mu_f, \mu) = \frac{m_f(\mu_f)}{m_q(\mu)}, \\
\Delta z_m^{fq}(x_{fq}) &= \frac{1}{24} \left(\frac{3}{2} l_{\mu_f} + 2 \right) x_{fq} \left\{ -24x_{fq}^3 \log^2(x_{fq}) - 12x_{fq} \log(x_{fq}) - 24x_{fq} \right. \\
&\quad + \pi^2 [(9 - 4x_{fq})x_{fq}^2 + 3] \\
&\quad + 6 [(4x_{fq} + 3)x_{fq}^2 + 1] [\log(x_{fq}) \log(x_{fq} + 1) + \text{Li}_2(-x_{fq})] \\
&\quad \left. + 6(x_{fq} - 1) [4x_{fq}^2 + x_{fq} + 1] [\log(1 - x_{fq}) \log(x_{fq}) + \text{Li}_2(x_{fq})] \right\}. \quad (26)
\end{aligned}$$

At the end of this Section we want to compare our result with the one of Ref. [14] where $z_m^{(3),M}$ has been computed in the linear approximation. Our result for the linear term reads

$$(M_f/m_q(m_q))^{(3),M}(x_q)|_{\text{linear}} = x_q \left[19.996 - 16.998 \log x_q + n_l (-1.039 + 1.097 \log x_q) \right]. \quad (27)$$

We find agreement for three of the terms but the coefficient with the numerical value 19.996 takes the value 21.277 in [14].⁴ This difference can be explained by the approximations performed in Ref. [14] in order to extract the linear term of the mass relation.⁵

4 Wave function renormalization constant

In contrast to Z_m^{OS} the wave function renormalization constant contains next to ultraviolet also infrared divergences. Thus it is not possible to construct a finite quantity by considering the ratio between the on-shell and $\overline{\text{MS}}$ renormalization constant. For this reason we discuss in what follows the coefficients of the ε -expansion separately.

4.1 Two-loop result

The two-loop corrections to $Z_2^{(2),M}$ have been computed in Ref. [3]. We confirmed this result and obtain

$$\begin{aligned}
Z_2^{(2),M} &= \frac{1}{\varepsilon} \left(\frac{1}{24} - \frac{1}{3} \log x \right) + \frac{1}{4} L_\mu^2 + \left(\frac{1}{6\varepsilon} + \frac{11}{36} - \frac{2}{3} \log x \right) L_\mu \\
&\quad + \frac{443}{432} + \frac{5\pi^2}{72} - \frac{\pi^2}{4} x + \frac{7}{6} x^2 - \frac{5\pi^2}{12} x^3 + \frac{\pi^2}{6} x^4
\end{aligned}$$

⁴Note that n_l as introduced in Ref. [14] corresponds to our combination $n_l + n_m$.

⁵We thank A. Hoang for communications on this point.

$$\begin{aligned}
& + \left(\frac{4}{9} + \frac{2}{3} x^2 \right) \log x + \left(\frac{2}{3} + x^4 \right) \log^2 x \\
& + \left(-\frac{1}{3} + \frac{1}{2} x + \frac{5}{6} x^3 - x^4 \right) [\log x \log(1-x) + \text{Li}_2(x)] \\
& - \left(\frac{1}{3} + \frac{1}{2} x + \frac{5}{6} x^3 + x^4 \right) [\log x \log(1+x) + \text{Li}_2(-x)] . \tag{28}
\end{aligned}$$

The convergence properties are very similar to $z_m^{(2),M}$ and shall not be discussed here. However, we would like to present a handy approximation formula which is obtained by an interpolation where the logarithmic divergence for $x \rightarrow 0$ is extracted before. It reads

$$\begin{aligned}
Z_2^{(2),M} &= \frac{1}{\varepsilon} \left(\frac{1}{24} - \frac{1}{3} \log x \right) + \frac{1}{4} L_\mu^2 + \left(\frac{1}{6\varepsilon} + \frac{11}{36} - \frac{2}{3} \log x \right) L_\mu \\
&+ \frac{2}{3} \log^2 x + \frac{4}{9} \log x + 1.711 - 2.356x + 1.125x^2 - 0.344x^3 . \tag{29}
\end{aligned}$$

and works to better than 1% for $x \in [0, 1]$.

4.2 Three-loop result

We again refrain from listing explicit results for the x -dependent coefficients and refer to the URL <http://www-ttp.physik.uni-karlsruhe.de/Progdata/ttp07/ttp07-21/> where the expressions can be downloaded in `Mathematica` format. It is, however, useful to present results for the analogue quantity to $z_m^{(3),M}$ as defined in Eq. (19). The cubic and quadratic poles can be presented analytically and read

$$\begin{aligned}
Z_2^{(3),M} \Big|_{\varepsilon^{-3}} &= \frac{1-\xi}{96} , \\
Z_2^{(3),M} \Big|_{\varepsilon^{-2}} &= -\frac{23}{108} - \frac{89}{96} L_\mu + \frac{19}{16} \log x + n_l \left(\frac{1}{108} + \frac{1}{36} L_\mu - \frac{1}{18} \log x \right) \\
&+ \xi \left(\frac{1}{32} - \frac{1}{32} L_\mu + \frac{1}{16} \log x \right) . \tag{30}
\end{aligned}$$

Concerning the single pole and the finite part we again present handy approximation formulae which we obtain by an interpolation to our expression after subtracting the singular terms for $x \rightarrow 0$. We cast the result in the form

$$\begin{aligned}
Z_2^{(3),M} \Big|_{\varepsilon^0} &= a_0 + a_1 L_\mu + a_2 L_\mu^2 + a_3 L_\mu^3 + \xi (b_0 + b_1 L_\mu + b_2 L_\mu^2 + b_3 L_\mu^3) , \\
Z_2^{(3),M} \Big|_{\varepsilon^{-1}} &= c_0 + c_1 L_\mu + c_2 L_\mu^2 + \xi (d_0 + d_1 L_\mu + d_2 L_\mu^2) , \tag{31}
\end{aligned}$$

where the coefficients are given by

$$\begin{aligned}
a_0 &= 0.38426 \log(x) [\log(x) + 0.53600] [\log(x) + 13.51219] \\
&\quad + 25.383 - 22.326x + 11.127x \log(x) - 1.473x^2, \\
a_1 &= \log(x) [-1.46528 \log(x) - 5.54630] + 6.832 - 1.971x + 0.982x^2 - 0.324x^3, \\
a_2 &= \frac{403}{288} \log(x) + \frac{127}{48}, \\
a_3 &= -\frac{193}{576}, \\
b_0 &= \frac{407}{864} + \frac{\pi^2}{128} - \frac{7\zeta(3)}{96} + \left(\frac{35}{48} + \frac{\pi^2}{64}\right) \log(x) + \frac{9}{16} \log^2(x) + \frac{3}{8} \log^3(x), \\
b_1 &= -\frac{35}{96} - \frac{\pi^2}{128} - \frac{9}{16} \log(x) - \frac{9}{16} \log^2(x), \\
b_2 &= \frac{9}{64} + \frac{9}{32} \log(x), \\
b_3 &= -\frac{3}{64}, \\
c_0 &= \log(x) [-1.34028 \log(x) - 2.41667] - 1.352 + 2.367x - 1.180x^2 + 0.387x^3, \\
c_1 &= \frac{23}{36} + \frac{257}{144} \log(x), \\
c_2 &= -\frac{41}{64}, \\
d_0 &= -\frac{35}{288} - \frac{\pi^2}{384} - \frac{3}{16} \log(x) - \frac{3}{16} \log^2(x), \\
d_1 &= \frac{3}{32} + \frac{3}{16} \log(x), \\
d_2 &= -\frac{3}{64}. \tag{32}
\end{aligned}$$

For the singular contributions, which we know to high precision, we provide five digits after the decimal point whereas for the results from the fit three digits are given.

As in the case of z_m we want to present the expanded results for $x \rightarrow 0$ which are given by ($\mu^2 = M_q^2$)

$$\begin{aligned}
Z_2^{(2),M} &= \frac{1}{\varepsilon} \left(\frac{1}{24} - \frac{1}{3} \log(x) \right) + \frac{443}{432} + \frac{5\pi^2}{72} + \frac{4}{9} \log(x) + \frac{2}{3} \log^2(x) \\
&\quad - \frac{\pi^2}{4} x + 2x^2 - \frac{5\pi^2}{12} x^3 + \left(\frac{125}{72} + \frac{\pi^2}{6} - \frac{11}{6} \log(x) + \log^2(x) \right) x^4 \\
&\quad + \left(-\frac{22}{75} + \frac{16}{45} \log(x) \right) x^6 + \left(-\frac{379}{7840} + \frac{3}{28} \log(x) \right) x^8, \tag{33} \\
Z_2^{(3),M} &= \frac{1}{\varepsilon^3} \left[0.0104 - 0.0104\xi \right]
\end{aligned}$$

$$\begin{aligned}
& + \frac{1}{\varepsilon^2} \left[-0.213 + (0.0093 - 0.0556L_x)n_l + 1.1875L_x + (0.0625L_x + 0.0313)\xi \right] \\
& + \frac{1}{\varepsilon} \left[-1.3978 + (0.0151 + 0.0741L_x + 0.0556L_x^2)n_l - 2.6389L_x - 1.5069L_x^2 \right. \\
& \quad + 2.4674x - 2x^2 + 4.1123x^3 + (-3.381 + 1.8333L_x - L_x^2)x^4 \\
& \quad + (0.2933 - 0.3556L_x)x^6 + (0.0483 - 0.1071L_x)x^8 \\
& \quad \left. + (-0.1472 - 0.1875L_x - 0.1875L_x^2)\xi \right] \\
& + 31.2973 + (-1.9715 + 0.1765L_x - 0.0741L_x^2 + 0.037L_x^3)n_l \\
& + 2.2534L_x + 5.6204L_x^2 + 0.2731L_x^3 \\
& + \left[-14.695 + 19.328L_x + (1.5578 - 1.6449L_x)n_l \right] x \\
& + (24.2836 - 0.7778n_l + 27.2951L_x - 0.6389L_x^2)x^2 \\
& + \left[-23.8364 + 28.4056L_x + (-2.7416L_x - 0.6021)n_l \right] x^3 \\
& + \left[-12.2965 + 7.3074L_x - 2.4541L_x^2 + 1.5787L_x^3 + (0.527 - 0.8466L_x \right. \\
& \quad \left. - 0.7222L_x^2 + 0.2222L_x^3)n_l \right] x^4 + (1.0836 + 1.7272n_l + 8.6633L_x)x^5 \\
& + \left[-2.8058 - 0.1342L_x + 3.125L_x^2 + 0.1389L_x^3 + (-0.7078 + 0.077L_x)n_l \right] x^6 \\
& + (0.4472 + 0.2937n_l + 1.6073L_x)x^7 + \left[-0.9511 + 0.8787L_x + 1.4563L_x^2 \right. \\
& \quad \left. + 0.0995L_x^3 + (-0.1831 + 0.0054L_x)n_l \right] x^8 \\
& + (0.4605 + 0.8834L_x + 0.5625L_x^2 + 0.375L_x^3)\xi. \tag{34}
\end{aligned}$$

In Fig. 5 we compare the exact results for the individual colour structures (for $\xi = 0$) with the approximations including terms up to order x^2 . Only for $x \gtrsim 0.2$ a difference is visible.

For completeness we show the analogue curves for the coefficient of the $1/\varepsilon$ pole in Fig. 6. It is interesting to mention that only Z_2^{FFM} has a non-trivial x -dependence beyond the logarithmic divergences for $x \rightarrow 0$.

5 Applications and conclusions

As an application of our result we want to discuss the charm quark effects in the relations between the pole, the $\overline{\text{MS}}$ and the $1S$ quark mass. For illustration we use $m_b(m_b) =$

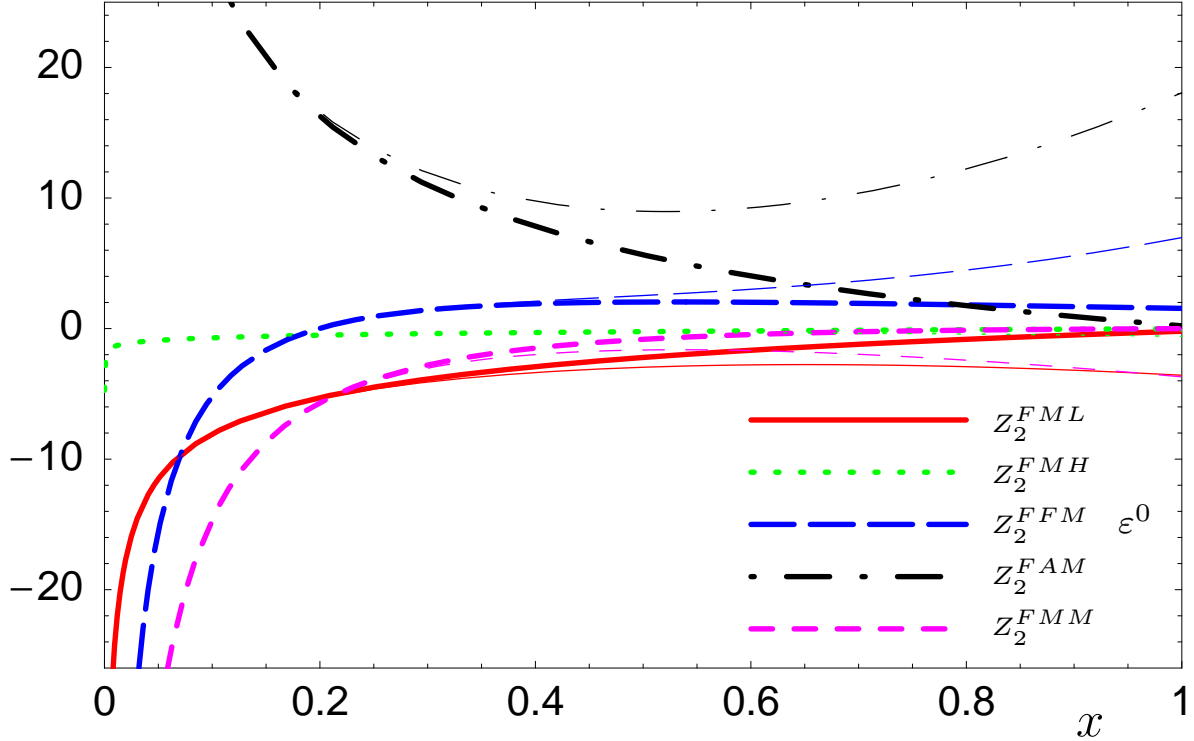


Figure 5: Finite parts of Z_2^{FML} , Z_2^{FMH} , Z_2^{FFM} , Z_2^{FAM} , Z_2^{FMM} for Feynman gauge ($\xi = 0$) and $L_\mu = 0$ as a function of x . The exact curves are represented by the thick and the small- x approximations by the thin lines.

4.2 GeV, $m_c(m_c) = 1.3$ GeV, $\mu = m_b$ and⁶ $\alpha_s^{(4)}(m_b) = 0.2247$. The relation between the on-shell and the $\overline{\text{MS}}$ mass leads to

$$M_b = \left[4.2 + 0.401 + \left(0.199 + 0.0094 \Big|_{m_c} \right) + \left(0.145 + 0.0182 \Big|_{m_c} \right) \right] \text{ GeV}, \quad (35)$$

where the tree-level, one-, two- and three-loop results are shown separately. The contributions from the charm quark mass which vanish for $m_c \rightarrow 0$ are marked by a subscript m_c . One observes that the higher order contributions are significant. In particular, the two-loop charm quark effects amount to 9 MeV and the three-loop ones to 18 MeV. A similar bad convergence is observed in the relation between the $1S$ mass [36] M_b^{1S} and the pole mass M_b . For $M_b = 4.8$ GeV, $m_c(m_c) = 1.3$ GeV, $\mu = M_b$ and $\alpha_s^{(4)}(M_b) = 0.2150$ it is given by

$$M_b^{1S} = \left[4.8 - 0.049 - \left(0.073 + 0.0041 \Big|_{m_c} \right) - \left(0.098 + 0.0112 \Big|_{m_c} \right) \right] \text{ GeV}. \quad (36)$$

⁶As a starting point we use $\alpha_s^{(5)}(M_Z) = 0.118$ and perform the running and decoupling with the program RunDec [35]. As in Ref. [36] we consider the mass relations with four active flavours.

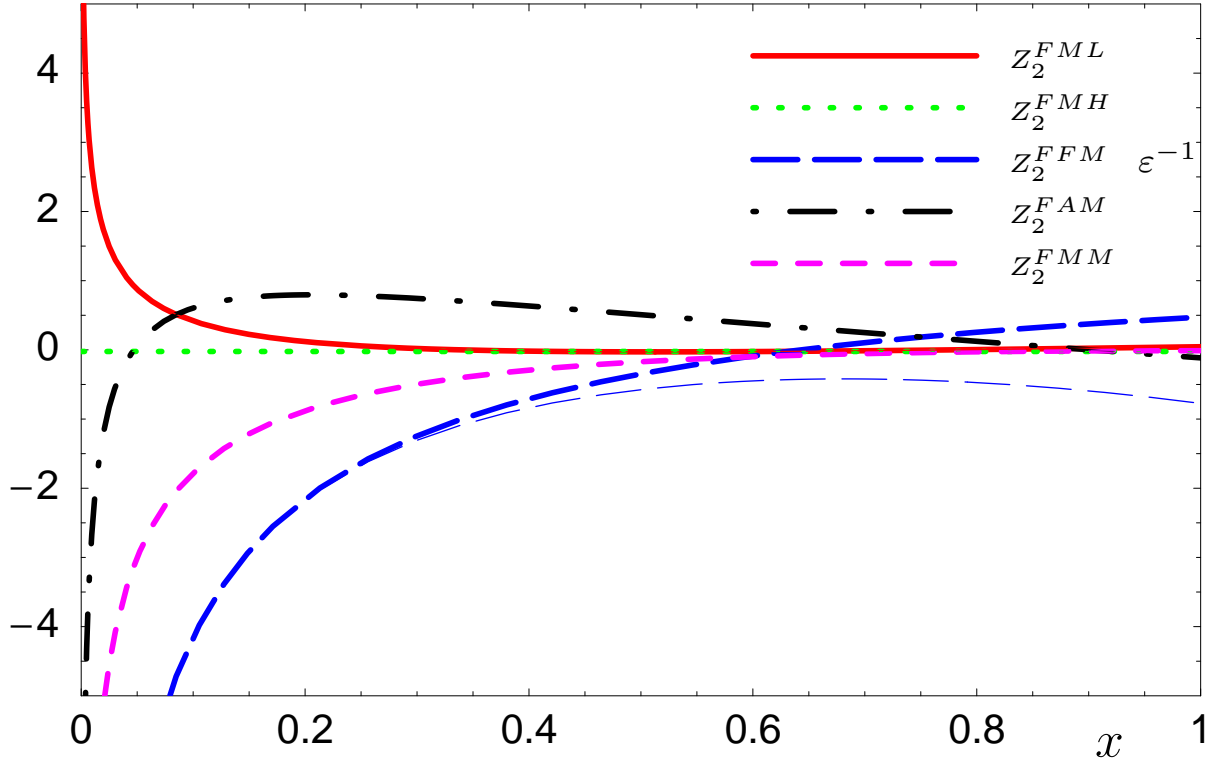


Figure 6: Same as in Fig. 5 but for the $1/\varepsilon$ pole.

However, the relation between the $1S$ and the $\overline{\text{MS}}$ quark mass is much better behaved as can be seen in the following example where we have chosen $M_b^{1S} = 4.69$ GeV, $m_c(m_c) = 1.3$ GeV, $\mu = M_b^{1S}$ and $\alpha_s^{(4)}(M_b^{1S}) = 0.2167$

$$m_b = \left[4.69 - 0.382 - \left(0.098 + 0.0047 \Big|_{m_c} \right) - \left(0.030 + 0.0051 \Big|_{m_c} \right) \right] \text{ GeV}. \quad (37)$$

The two-loop charm effects amount to only 4.7 MeV and three-loop ones to 5.1 MeV. We want to mention that in case only the linear approximation [14] of the charm quark mass effects is used the corresponding three-loop results in Eqs. (35) and (37) read 0.0167 and 0.0037, respectively.

We are now in the position to compare with Eq. (168) of Ref. [14] which provides the relation between the $1S$ and $\overline{\text{MS}}$ bottom quark mass allowing for a variation of M_b^{1S} , m_c , α_s and the renormalization scale μ . Updating the coefficient of the m_c term one obtains the formula

$$m_b = 4.169 \text{ GeV} - 0.009 (m_c(m_c) - 1.4 \text{ GeV}) \quad (38)$$

which has an accuracy of better than 0.01% for $1.1 \text{ GeV} < m_c < 1.7 \text{ GeV}$.

A further application of our result would be the incorporation of our corrections in the analysis of the bottom quark mass determination from the $\Upsilon(1S)$ system. In the analysis performed in Ref. [37] the charm quark mass has not been considered and an uncertainty of ± 10 MeV has been assigned which could be reduced to a large extent.

To conclude, in this paper we have computed the three-loop QCD corrections to the on-shell renormalization constants for a heavy quark mass and the corresponding wave function where a second massive quark appears in closed loops. The two-scale three-loop diagrams are analytically reduced to 27 master integrals. The ε -expansion of the latter is computed in analytical form, except for six coefficients for which one- and two-dimensional integral representations are available. We derived a compact expansion of the renormalization constants in the limit where the second quark mass is small. A rapid convergence is observed providing a good approximation to the exact result even close to the equal-mass case.

Acknowledgements

We thank V.A. Smirnov for cross checks on some of the intermediate results. This work was supported by the DFG through SFB/TR 9 and the Graduiertenkolleg ‘‘Hochenergiephysik und Teilchenastrophysik’’.

A Master integrals

In this Appendix we collect the master integrals appearing in our calculation in graphical form.

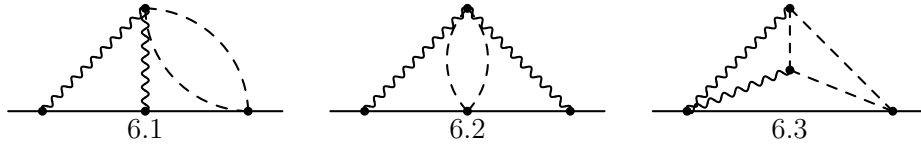


Figure 7: Three-loop master integrals with six lines. Solid and dashed lines denote massive lines with masses m_q and m_f , respectively. Wavy lines are massless scalar propagators.

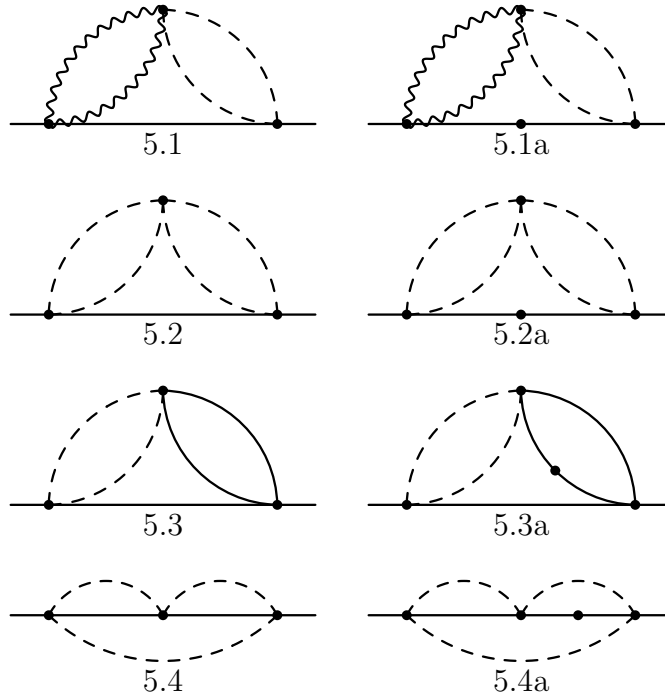


Figure 8: Three-loop master integrals with five lines.

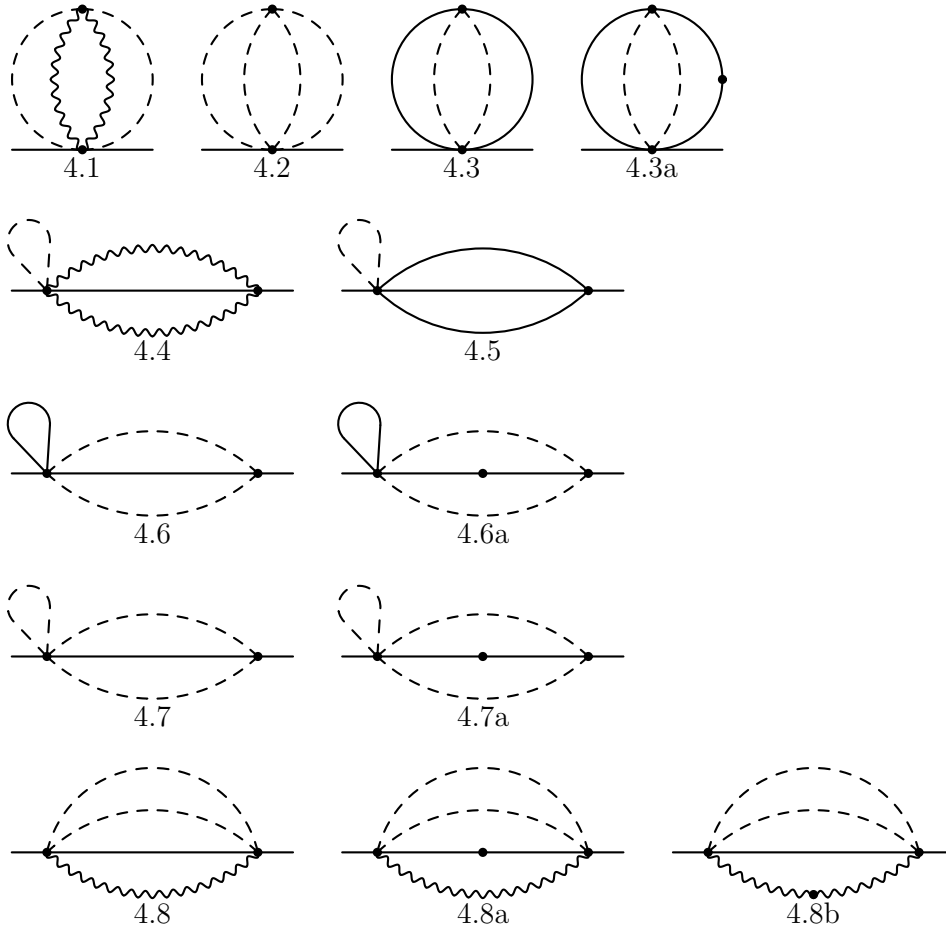


Figure 9: Three-loop master integrals with four lines.

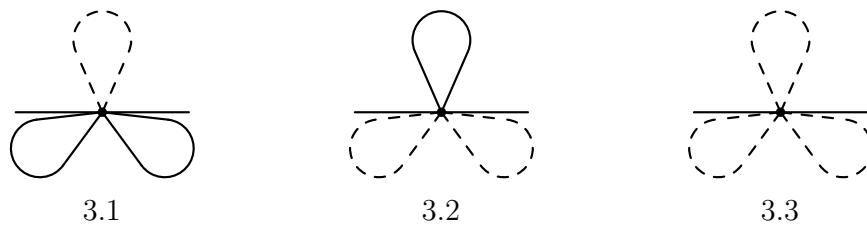


Figure 10: Three-loop master integrals with three lines.

References

- [1] R. Tarrach, Nucl. Phys. B **183** (1981) 384.

- [2] N. Gray, D. J. Broadhurst, W. Grafe and K. Schilcher, *Z. Phys. C* **48** (1990) 673.
- [3] D. J. Broadhurst, N. Gray and K. Schilcher, *Z. Phys. C* **52** (1991) 111.
- [4] D. J. Broadhurst, *Z. Phys. C* **54** (1992) 599.
- [5] D. J. Broadhurst, arXiv:hep-th/9604128.
- [6] A. I. Davydychev and A. G. Grozin, *Phys. Rev. D* **59** (1999) 054023 [arXiv:hep-ph/9809589].
- [7] M. Argeri, P. Mastrolia and E. Remiddi, *Nucl. Phys. B* **631**, 388 (2002) [arXiv:hep-ph/0202123].
- [8] A. Onishchenko and O. Veretin, *Phys. Atom. Nucl.* **68** (2005) 1405 [*Yad. Fiz.* **68** (2005) 1461] [arXiv:hep-ph/0207091].
- [9] K. G. Chetyrkin and M. Steinhauser, *Phys. Rev. Lett.* **83** (1999) 4001 [arXiv:hep-ph/9907509].
- [10] K. G. Chetyrkin and M. Steinhauser, *Nucl. Phys. B* **573** (2000) 617 [arXiv:hep-ph/9911434].
- [11] K. Melnikov and T. van Ritbergen, *Phys. Lett. B* **482** (2000) 99 [arXiv:hep-ph/9912391].
- [12] K. Melnikov and T. van Ritbergen, *Nucl. Phys. B* **591** (2000) 515 [arXiv:hep-ph/0005131].
- [13] P. Marquard, L. Mihaila, J. H. Piclum and M. Steinhauser, *Nucl. Phys. B* **773** (2007) 1 [arXiv:hep-ph/0702185].
- [14] A. H. Hoang, arXiv:hep-ph/0008102.
- [15] M. Melles, *Phys. Rev. D* **62** (2000) 074019 [arXiv:hep-ph/0001295].
- [16] O. V. Tarasov,
- [17] E. Remiddi and J. A. M. Vermaseren, *Int. J. Mod. Phys. A* **15** (2000) 725 [arXiv:hep-ph/9905237].
- [18] P. Nogueira, *J. Comput. Phys.* **105** (1993) 279.
- [19] R. Harlander, T. Seidensticker and M. Steinhauser, *Phys. Lett. B* **426** (1998) 125 [hep-ph/9712228].
- [20] T. Seidensticker, hep-ph/9905298.
- [21] A. G. Grozin, A. V. Smirnov and V. A. Smirnov, *JHEP* **0611** (2006) 022 [arXiv:hep-ph/0609280].

- [22] S. Laporta and E. Remiddi, Phys. Lett. B **379** (1996) 283 [arXiv:hep-ph/9602417].
- [23] S. Laporta, Int. J. Mod. Phys. A **15** (2000) 5087 [arXiv:hep-ph/0102033].
- [24] P. Marquard and D. Seidel, unpublished.
- [25] C. Bauer, A. Frink and R. Kreckel, arXiv:cs.sc/0004015.
- [26] R. H. Lewis, Fermat's User Guide, <http://www.bway.net/~lewis>.
- [27] M. Tentyukov and J. A. M. Vermaseren, arXiv:cs.sc/0604052.
- [28] K. G. Chetyrkin and F. V. Tkachov, Nucl. Phys. B **192** (1981) 159.
- [29] V. A. Smirnov, Springer Tracts Mod. Phys. **211** (2004) 1.
- [30] M. Czakon, Comput. Phys. Commun. **175** (2006) 559 [arXiv:hep-ph/0511200].
- [31] A. V. Kotikov, Phys. Lett. B **254** (1991) 158.
- [32] S. Bekavac, A. Grozin, D. Seidel, A.V. Smirnov, in preparation.
- [33] D. Maitre, Comput. Phys. Commun. **174** (2006) 222 [arXiv:hep-ph/0507152].
- [34] D. Maitre, arXiv:hep-ph/0703052.
- [35] K. G. Chetyrkin, J. H. Kühn and M. Steinhauser, Comput. Phys. Commun. **133** (2000) 43 [arXiv:hep-ph/0004189].
- [36] A. H. Hoang, M. C. Smith, T. Stelzer and S. Willenbrock, Phys. Rev. D **59** (1999) 114014 [arXiv:hep-ph/9804227].
- [37] A. A. Penin and M. Steinhauser, Phys. Lett. B **538** (2002) 335 [arXiv:hep-ph/0204290].